IMMUNOLOGY

YAP-mediated mechanotransduction tunes the macrophage inflammatory response

Vijaykumar S. Meli[1,2], Hamza Atcha[1,2]*, Praveen Krishna Veerasubramanian[1,2]*, Raji R. Nagalla[1,2]*, Thuy U. Luu[2,3], Esther Y. Chen[2,4], Christian F. Guerrero-Juarez[5,6,7,8,9], Kosuke Yamaga[5,6,7,9], William Pandori[10,11], Jessica Y. Hsieh[1,2], Timothy L. Downing[1,2,6,7,9,12], David A. Fruman[10,11], Melissa B. Lodoen[10,11], Maksim V. Plikus[5,6,7,9], Wenqi Wang[5], Wendy F. Liu[1,2,4,11†]

Copyright © 2020 The Authors, some rights reserved; exclusive licensee American Association for the Advancement of Science. No claim to original U.S. Government Works. Distributed under a Creative Commons Attribution NonCommercial License 4.0 (CC BY-NC).

Macrophages are innate immune cells that adhere to the extracellular matrix within tissues. However, how matrix properties regulate their function remains poorly understood. Here, we report that the adhesive microenvironment tunes the macrophage inflammatory response through the transcriptional coactivator YAP. We find that adhesion to soft hydrogels reduces inflammation when compared to adhesion on stiff materials and is associated with reduced YAP expression and nuclear localization. Substrate stiffness and cytoskeletal polymerization, but not adhesive confinement nor contractility, regulate YAP localization. Furthermore, depletion of YAP inhibits macrophage inflammation, whereas overexpression of active YAP increases inflammation. Last, we show in vivo that soft materials reduce expression of inflammatory markers and YAP in surrounding macrophages when compared to stiff materials. Together, our studies identify YAP as a key molecule for controlling inflammation and sensing stiffness in macrophages and may have broad implications in the regulation of macrophages in health and disease.

INTRODUCTION

Macrophages are essential cells of the innate immune system recognized for critical roles in defense against pathogens, as well as during development, homeostasis, and tissue repair. Some of the many macrophage functions include clearing of pathogens or apoptotic cells and debris, promoting and resolving inflammation, facilitating tissue patterning, and healing after injury (*1*, *2*). To perform this multitude of functions, macrophages have an exquisite ability to sense and respond to signals in their microenvironment. For example, inflammatory cytokines and pathogens polarize macrophages toward a classically activated phenotype to promote inflammation. In response to wound-healing cytokines such as interleukin-4 (IL-4) and IL-13, the same cells can polarize toward healing phenotypes and function to dampen inflammation, promote angiogenesis, and facilitate tissue repair. Perhaps because of their many roles in maintaining health, macrophage dysfunction is associated with numerous diseases including cancer, cardiovascular disease, and fibrosis (*1*). Notably, all of these conditions are also characterized by remodeling of the extracellular matrix (ECM) and often increases in tissue stiffness, which itself is known to regulate cell function (*3*). Work from the past decade has tremendously expanded our knowledge about how macrophages respond to soluble, diffusible signals in their environment. However, although these cells reside in tissues that are rich in mechanical cues, there is still very little known about the molecular mechanisms of how physical cues, such as environmental stiffness, control their phenotype.

Our group and others have found that adhesion to soft ECM hydrogels (<1 kPa) inhibits macrophage inflammatory activation when compared to adhesion to stiff glass or polystyrene culture dishes (~GPa) (*4*, *5*). Given that persistent macrophage inflammation is associated with scar formation, this effect is consistent with reports showing that stiffer materials promote fibrosis after implantation (*6*, *7*). Toll-like receptor 4 (TLR4)–associated signaling has been shown to be mechanically regulated (*7*), but the overall molecular mechanisms underlying mechanotransduction in macrophages remain relatively unknown. In many adhesive cell types, transduction of mechanical cues into biochemical signals is thought to involve integrin clustering, cytoskeletal contractility, and associated signaling pathways (*8*–*14*). Mechanical cues have also been linked to the activity of transcriptional coactivators Yes-associated protein (YAP) and transcriptional coactivator with PDZ-binding motif (TAZ), establishing a connection between extracellular biophysical cues and gene regulation (*15*–*19*). In hematopoietic cells, YAP expression is thought to be low, but a few studies have shown that YAP is involved in monocyte adhesion to inflamed endothelium and macrophage activation (*20*–*25*). Manipulation of YAP/TAZ is currently being explored as a therapeutic approach for a wide range of pathologies that involve macrophages and exhibit prominent changes in the biophysical tissue environment (*23*, *26*, *27*). However, there is currently no reported role of YAP/TAZ in the regulation of macrophages by biophysical cues.

Here, we show that the biophysical microenvironment tunes the macrophage inflammatory response through YAP. We find that YAP is dynamically sensitive to substrate stiffness and enters the nucleus upon adhesion to stiff surfaces. Moreover, nuclear YAP enhances the

[1]Department of Biomedical Engineering, University of California, Irvine, Irvine, CA, USA. [2]Edwards Lifesciences Center for Advanced Cardiovascular Technology, University of California, Irvine, Irvine, CA, USA. [3]Department of Pharmaceutical Sciences, University of California, Irvine, Irvine, CA, USA. [4]Department of Chemical and Biomolecular Engineering, University of California, Irvine, Irvine, CA, USA. [5]Department of Developmental and Cell Biology, University of California, Irvine, Irvine, CA, USA. [6]NSF–Simons Center for Multiscale Cell Fate Research, University of California, Irvine, Irvine, CA, USA. [7]Sue and Bill Gross Stem Cell Research Center, University of California, Irvine, Irvine, CA, USA. [8]Department of Mathematics, University of California, Irvine, Irvine, CA 92697, USA. [9]Center for Complex Biological Systems, University of California, Irvine, Irvine, CA 92697, USA. [10]Department of Molecular Biology and Biochemistry, University of California, Irvine, Irvine, CA, USA. [11]Institute for Immunology, University of California, Irvine, Irvine, CA, USA. [12]Department of Microbiology and Molecular Genetics, University of California, Irvine, Irvine, CA, USA.
*These authors contributed equally to this work.
†Corresponding author. Email: wendy.liu@uci.edu

macrophage response to the inflammatory agonist lipopolysaccharide (LPS). Cytoskeletal polymerization is required for YAP nuclear localization, but active YAP negatively feeds back to inhibit actin, adhesion, and traction forces. Last, we show that stiff biomaterial implants enhance macrophage YAP and fibrosis when compared to soft implants. Our findings identify a new molecular target capable of regulating macrophage responses within different stiffness environments.

RESULTS

Adhesion to fibrin inhibits inflammatory activation of macrophages

We previously found that culture of murine bone marrow macrophages on fibrin hydrogels inhibited tumor necrosis factor–α (TNFα) secretion in response to inflammatory stimuli when compared to cells cultured on polystyrene, whereas its soluble precursor fibrinogen enhanced TNFα secretion (*4*). We further sought to examine the response in human cells and to investigate the underlying mechanisms of immunomodulation by the ECM. We compared cells seeded on a very soft ECM hydrogel with cells cultured on standard tissue culture polystyrene. Primary human macrophages were differentiated from peripheral blood monocytes, seeded on fibrin hydrogels or tissue culture polystyrene surfaces overnight, and stimulated with LPS and/or fibrinogen for 6 hours, and then, supernatant was collected to measure secreted cytokine levels. We found that culture on fibrin inhibited TNFα secretion upon activation by LPS, but addition of soluble fibrinogen exerted minimal effects (fig. S1A). The human monocyte/macrophage cell line THP-1 also exhibited an inhibition of inflammatory activation when differentiated with phorbol myristate acetate (PMA) and stimulated with LPS on fibrin hydrogels. However, in contrast to primary cells, fibrinogen enhanced TNFα secretion in THP-1 cells seeded on polystyrene, both with and without LPS stimulation (fig. S1B), similar to our earlier report (*4*). Furthermore, inhibition of TNFα was observed across a range of LPS dosages (fig. S1, C and D) and many TLR agonists including Pam3CSK4 (TLR1/2 agonist) and FSL-1 (TLR6/2 agonist) (fig. S2A). To further examine the inhibition of inflammatory activation by adhesion to fibrin, we probed several additional cytokines and found that fibrin inhibited not only LPS-induced secretion of TNFα but also IL-6 and MCP-1 (monocyte chemoattractant protein-1) and up-regulated the anti-inflammatory cytokine IL-10, when compared to cells cultured on polystyrene control surfaces (Fig. 1A), suggesting that adhesion to fibrin hydrogels broadly inhibits inflammatory activation of macrophages.

To examine whether regulation by the ECM occurs at the gene level, we analyzed expression of *TNF*, *IL6*, *MCP1*, and *IL10* by reverse transcription polymerase chain reaction (RT-PCR) in human macrophages cultured on fibrin or polystyrene and stimulated with LPS for 4 hours. Similar to their secretion, *TNF* and *IL6* expression were inhibited and *IL10* expression increased when cells were cultured on fibrin and stimulated with LPS, compared to cells cultured on polystyrene (Fig. 1B). However, no differences in *MCP1* mRNA amounts were observed in cells cultured on fibrin compared to polystyrene at this time point and *IL10* expression increased in cells on fibrin even without LPS stimulation (Fig. 1B). Analysis of a panel of inflammatory genes using multiplex gene expression platform from NanoString revealed several additional genes that were differentially regulated by culture on fibrin versus polystyrene and/or stimulation with LPS (fig. S2B).

Regulation of nuclear factor κB and YAP by adhesion and activation

To examine potential transcriptional regulators of macrophage behavior in different adhesive environments, we investigated nuclear factor kappa light-chain enhancer of activated B cells (NF-κB) and YAP, which have been shown to be involved in inflammation and mechanosensing, respectively (*15*, *28*). Macrophages were seeded on fibrin hydrogel–coated or plain glass to enable visualization by immunofluorescence microscopy, and NF-κB and YAP localization were examined before and after 1 hour of stimulation with LPS. We observed that both NF-κB (p65 domain) and YAP were modulated by adhesion to hydrogels, with less total intensity and nuclear localization in cells cultured on fibrin compared to cells cultured on glass (Fig. 1, C and D). Stimulation with LPS increased nuclear localization of NF-κB p65 in cells cultured on both surfaces, although the increase was much more substantial in cells cultured on polystyrene. In contrast, LPS induced a much smaller increase in nuclear YAP. Since hematopoietic cells are thought to have low YAP expression, we examined whether differentiation from monocytes to macrophages might influence YAP expression. We found that YAP protein levels increased as monocytes differentiated to macrophages with macrophage colony-stimulating factor (M-CSF; fig. S3A). Gene expression of the YAP paralog *TAZ* was relatively stable during differentiation, and expressions of *YAP* and *TAZ* were similar after 7 days of differentiation (fig. S3, B to D).

NF-κB and YAP activity are both regulated by phosphorylation, where NF-κB phosphorylation is associated with activation and required for nuclear entry upon LPS stimulation, and conversely, YAP phosphorylation leads to its degradation in the cytoplasm and is associated with inactivity. We performed Western blotting to probe for phosphorylated and total transcription factor levels in cells cultured on fibrin and polystyrene. We observed a moderate increase in total NF-κB and a significant increase in phosphorylated NF-κB in cells on polystyrene compared to fibrin, and LPS induced an increase in phosphorylation only in cells on polystyrene surfaces (Fig. 1E). We observed lower total YAP and higher YAP phosphorylation in cells cultured on fibrin when compared to polystyrene (Fig. 1F and fig. S4). Furthermore, levels of YAP phosphorylation did not appear to be affected by LPS. We observed similar effects of adhesion and stimulation on nuclear localization of TAZ (fig. S5A) and YAP in THP-1 and U937 human monocyte/macrophage cells treated with PMA (fig. S5, B and C). Together, these data suggest that while NF-κB signaling appears to be mostly influenced by inflammatory signals such as LPS, YAP signaling is predominantly regulated by the adhesive microenvironment and its presence in the nucleus could potentially tune inflammatory activation of macrophages.

YAP dynamically increases upon differentiation and adhesion to stiff surfaces

To further examine how the dynamics of adhesion influences YAP nuclear translocation, we cultured macrophages on fibrin or glass and stained for YAP over a time course following seeding. We observed that at early time points (1 hour), YAP was highly expressed and localized both outside and within the nucleus in cells on glass, and expression was lower in cells cultured on fibrin (Fig. 2A). As adhesion continued on glass, YAP progressively translocated into the nucleus. In contrast, YAP remained excluded from the nucleus in cells cultured on fibrin and appeared to degrade over time with overall expression levels decreasing and phosphorylation increasing

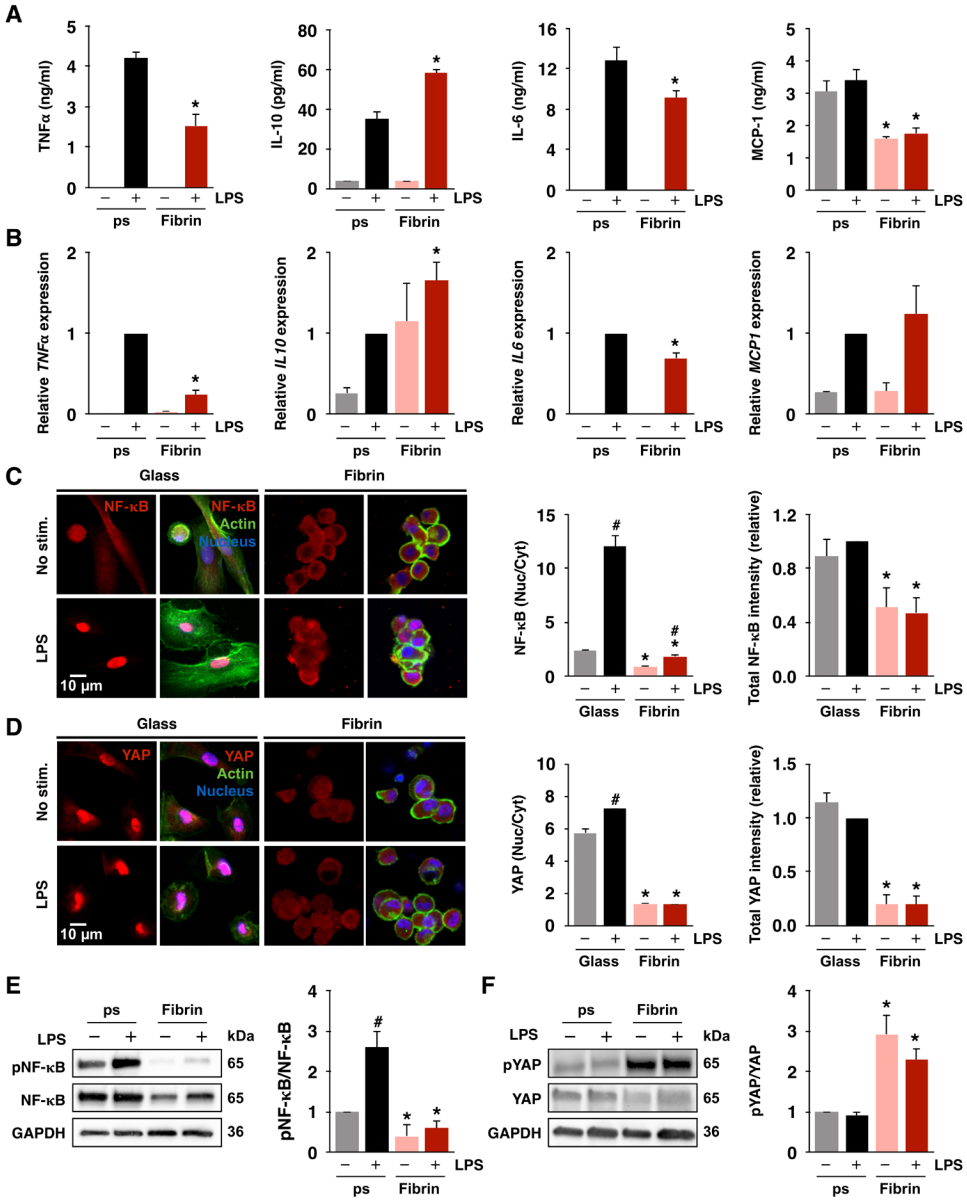

Fig. 1. Culture substrate modulates macrophage inflammatory activation, NF-κB, and YAP. (**A**) Cytokine secretion by monocyte-derived macrophages cultured on fibrin gels (2 mg/ml) or polystyrene (ps), stimulated with LPS (10 ng/ml), measured by enzyme-linked immunosorbent assay (ELISA). (**B**) Relative expression of genes in (A) analyzed by quantitative PCR (qPCR), normalized to polystyrene with LPS. (**C**) Immunofluorescence confocal images of NF-κB (left) in monocyte-derived macrophages cultured on glass or fibrin (2 mg/ml) for 24 hours and stimulated with LPS for 1 hour and quantification of nuclear/cytoplasmic ratio and total NF-κB intensities (right). (**D**) Immunofluorescence confocal images of YAP (left) and quantification of nuclear/cytoplasmic ratio and total YAP intensities (right) of the same conditions shown in (C). (**E**) Immunoblots and quantification of NF-κB and phosphorylated NF-κB (pNF-κB) in monocyte-derived macrophages as in (C). (**F**) Immunoblots and quantification of YAP and phosphorylated YAP (pYAP; S127) in macrophages cultured as in (C). For immunoblots and immunostaining, quantification is an average of three blots or at least 150 cells across three biological replicates, respectively. All the values are means ± SEM; **P* < 0.05 when comparing fibrin to polystyrene or glass with the same soluble condition and #*P* < 0.05 when comparing LPS to no LPS with the same substrate condition, assessed by two-tailed Student's *t* test. GAPDH, glyceraldehyde-3-phosphate dehydrogenase.

(Fig. 2, A and B). Analysis of canonical YAP target genes did not reveal any increase in their expression as time of adhesion and YAP nuclear localization increased on polystyrene, suggesting potentially unique targets for YAP in macrophages (fig. S6A). Immunostaining of histone modifications that are associated with accessible chromatin states including histone acetylation (H3Ac) and methylation (H3K4me3) showed a similar pattern to YAP, with significantly higher global staining intensity in the nuclei of cells cultured on glass compared to cells cultured on fibrin (fig. S6, B and C). These data suggest that additional gene regulatory network events may be involved and a potential association between YAP and chromatin remodeling. To determine whether adhesion-modulated changes in YAP nuclear localization might alter their response to LPS, we compared stimulated cells that were adhered for only 1 hour to cells adhered overnight

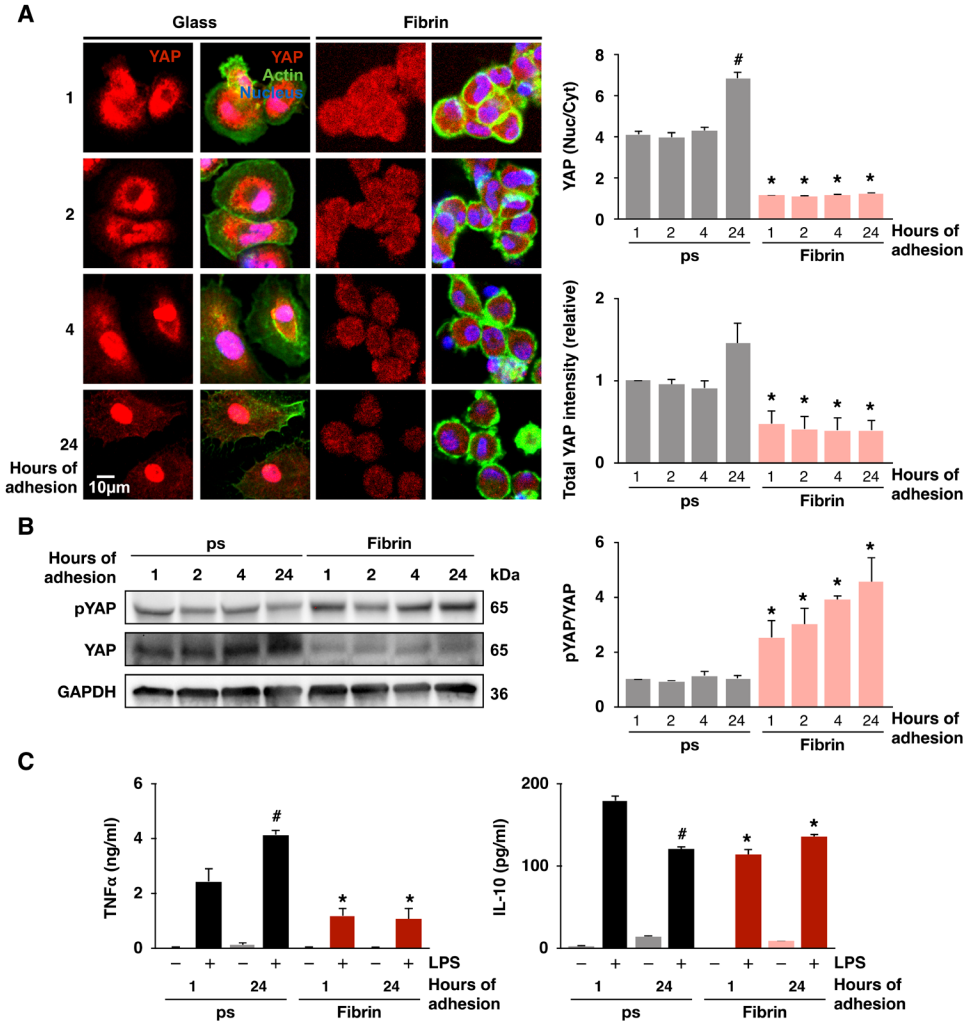

Fig. 2. Adhesion dynamically regulates YAP nuclear translocation and inflammation. (**A**) Immunofluorescence confocal images of YAP in monocyte-derived macrophages cultured on glass or fibrin hydrogels (2 mg/ml) for 1, 2, 4, and 24 hours (left) and quantification of nuclear-to-cytoplasmic ratio and total intensity (right). (**B**) Immunoblot of phosphorylated and total YAP at 1, 2, 4, and 24 hours after adhesion (left) and quantification of phosphorylated to total YAP ratio (right). (**C**) Secretion of TNFα and IL-10 by monocyte-derived macrophages cultured on polystyrene or fibrin hydrogels (2 mg/ml) for 1 or 24 hours and then stimulated with LPS (10 ng/ml) for 6 hours, analyzed by ELISA. Immunoblots and cytokines are quantified across three separate blots/biological replicates. For immunostaining, analysis was performed on at least 150 cells across three biological replicates at each time point. Data are presented as means ± SEM; *$P < 0.05$ when comparing fibrin to glass or polystyrene and #$P < 0.05$ when comparing 1 hour versus 24 hours of adhesion, assessed by two-tailed Student's t test.

for 24 hours. We found that LPS-induced activation of cells that had adhered for only 1 hour led to less TNFα and more IL-10 secretion when compared to cells adhered for 24 hours (Fig. 2C). These data show that YAP nuclear localization is dynamically influenced by adhesion and is associated with enhanced inflammatory activation.

Regulation of YAP by mechanical stiffness and adhesive confinement

We next probed whether the observed differences in inflammation and YAP nuclear localization could be recapitulated on other hydrogel materials and whether the differences are caused by changes in mechanical stiffness of the environment since fibrin is very soft (~100 Pa) and glass or polystyrene is very stiff (~GPa). Cells were cultured on collagen, Matrigel, and polyethylene glycol (PEG) and stimulated with varying doses of LPS. On all hydrogel materials, macrophages secreted less TNFα compared to cells on polystyrene controls (fig. S7A). Furthermore, cells cultured on collagen also exhibited less YAP nuclear localization compared to cells on glass (fig. S7B). To investigate the role of stiffness, cells were cultured on fibrinogen-conjugated synthetic polyacrylamide hydrogels, with varied cross-linking density to modulate stiffness (*29*). We found that on low-stiffness (1 kPa) substrates, YAP was distributed throughout the nucleus and cytoplasm, and as the stiffness increased to 20 and 280 kPa, YAP nuclear localization gradually increased (Fig. 3A), consistent with many other cell types (*30*, *31*). LPS-induced TNFα secretion again correlated directly with YAP nuclear localization, with higher levels in cells cultured on stiff surfaces compared to cells cultured on soft surface (Fig. 3B). However unlike on fibrin surfaces, culture of macrophages on soft 1-kPa polyacrylamide surfaces did not enhance IL-10 secretion, suggesting that this response may require stiffness <1 kPa or ligand

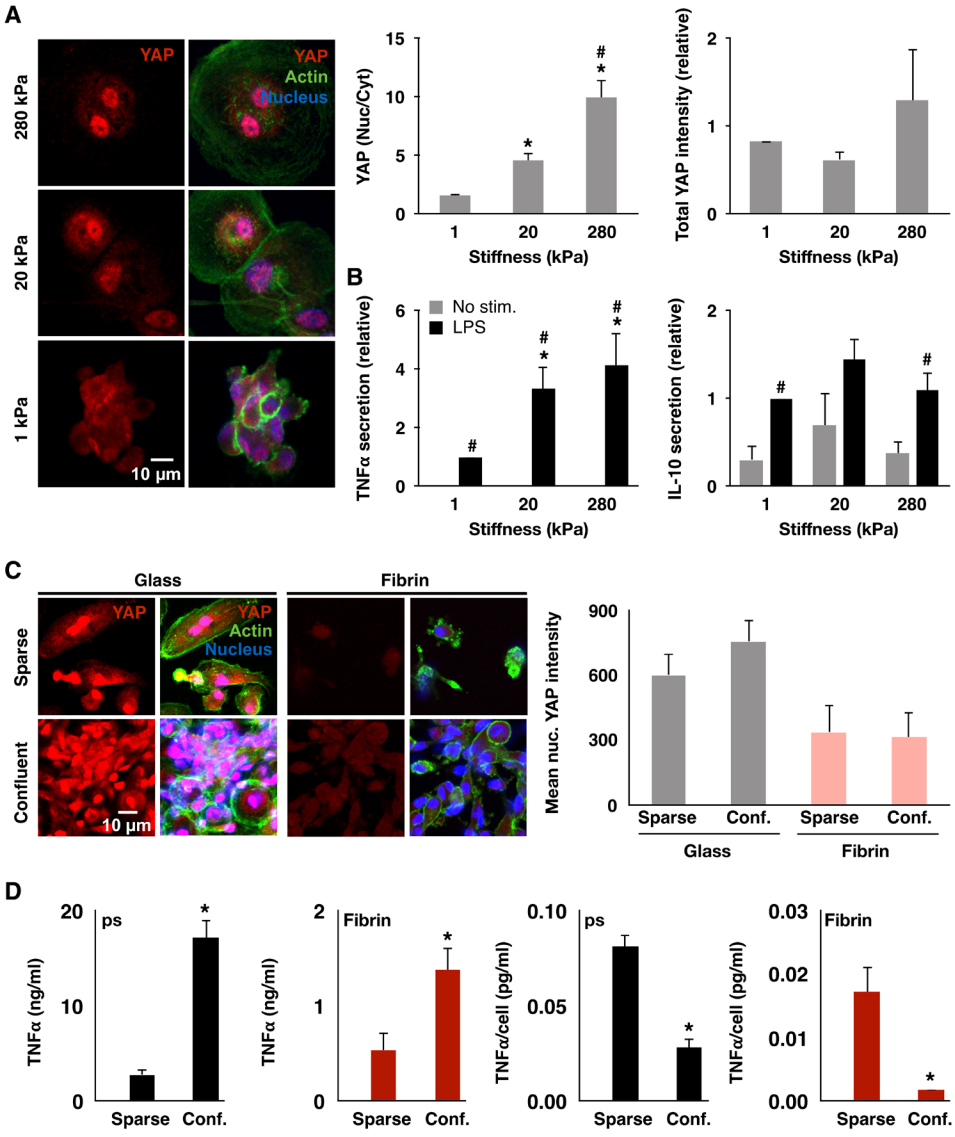

Fig. 3. Substrate stiffness, but not cell confinement, modulates YAP nuclear localization and inflammation. (**A**) Immunofluorescence confocal images of YAP in monocyte-derived macrophages cultured on polyacrylamide gels of varying stiffness for 24 hours and stimulated with LPS (10 ng/ml) for 6 hours (left) and quantification of nuclear to cytoplasmic ratio and total intensity (right). (**B**) Cytokine secretion from cells in (A) analyzed by ELISA. (**C**) Immunofluorescence confocal images of YAP in monocyte-derived macrophages cultured on glass at low (0.02 million cells/cm^2) or high (0.33 million cells/cm^2) seeding density (left) and quantification of mean nuclear YAP intensity (right). (**D**) Secretion of TNFα and IL-10 of cells in (C) and stimulated with LPS (10 ng/ml) for 6 hours, analyzed by ELISA. Immunostaining analysis was performed on at least 150 cells across three biological replicates. Values are means ± SEM of three biological replicates; *$P < 0.05$ when comparing 1 to 20 kPa or 280 kPa and #$P < 0.05$ when comparing 20 and 280 kPa in (A), *$P < 0.05$ comparing 1 to 20 kPa or 280 kPa and #$P < 0.05$ when comparing LPS to no LPS in (B), and *$P < 0.05$ when comparing high versus low cell density in (C), assessed by two-tailed Student's *t* test.

and fibrillar architectures that are only achieved with native ECM hydrogels.

Since cells cultured on fibrin exhibited considerably less spreading when compared to cells on glass (Fig. 1, C and D) and cell confinement has been shown to be another regulator of YAP activity, we also examined whether restricting cell spreading influenced YAP and inflammatory activation in macrophages. Using microcontact printing, we created patterns of 400-μm^2 adhesive fibrinogen islands on stiff polydimethylsiloxane surfaces, which were similar in size to the area of the cells cultured on fibrin. In addition, we cultured the cells at high densities to induce cell crowding and to investigate the role of YAP in cell contact inhibition in macrophages (Fig. 3C). After culture on micropatterned or dense conditions for 24 hours, we found that neither method of cell confinement influenced nuclear YAP when compared to cells seeded sparsely (Fig. 3C and fig. S7C). Patterned cells did not provide sufficient cell numbers for analysis of cytokine secretion, but comparing the activation of confluent versus subconfluent cells showed higher overall TNFα levels when cells were confluent (Fig. 3D). However, normalizing the total levels by the number of cells in the culture well shows that the average TNFα secreted by individual cells at confluence is lower than that at subconfluence (Fig. 3D), suggesting that

YAP-independent mechanisms for inhibiting inflammation also exist. Nonetheless, these data show that YAP activity is dependent on material stiffness, but not adhesive confinement or cell crowding, in macrophages.

YAP activity tunes macrophage response to inflammatory stimuli

Our data suggest that the macrophage response to inflammatory stimuli depends on nuclear YAP and its exclusion from the nucleus protects the cells from inflammation. To test this hypothesis, we examined whether knockdown or expression of constitutively active YAP alters macrophage inflammatory activation. Knockdown of YAP with small interfering RNA (siRNA) reduced YAP nuclear staining by approximately 40% and gene expression levels by greater than 60%, compared to control cells treated with a control siRNA sequence that has no known target in human genome (Fig. 4A and fig. S8A). Stimulation of siRNA-treated cells with LPS showed reduced TNFα secretion compared to nontarget controls (Fig. 4B). Knockdown of TAZ with siRNA achieved greater than 50% knockdown at the gene level and also reduced LPS-induced TNFα secretion, although to a lesser extent than YAP (Fig. 4B). We then transduced a lentivirus expressing YAP-5SA, the constitutively active mutant that is resistant to phosphorylation and degradation, and a YAP-specific short hairpin RNA plasmid (shYAP) construct that causes constitutive knockdown of YAP expression in THP-1 cells. YAP-5SA–expressing cells were found to have enhanced YAP staining across the entire cell and higher gene expression, whereas shYAP showed significantly reduced expression of gene and protein compared to cells transduced with a control vector (Fig. 4, C and E). While YAP immunostaining was difficult to quantify because of high expression levels, detection of transgene by Western blot revealed the 65-kDa native YAP along with a higher intensity 75-kDa band indicating YAP-5SA overexpression, due to a C-terminal fusion of SFB tag, and a significantly diminished band in shYAP-expressing cells (Fig. 4D). Furthermore, LPS induced significantly higher TNFα secretion in YAP-5SA–expressing macrophages cultured on both polystyrene and fibrin when compared to a control vector and significantly lower TNFα secretion in shYAP macrophages cultured on polystyrene (Fig. 4F). Similar observations were made in

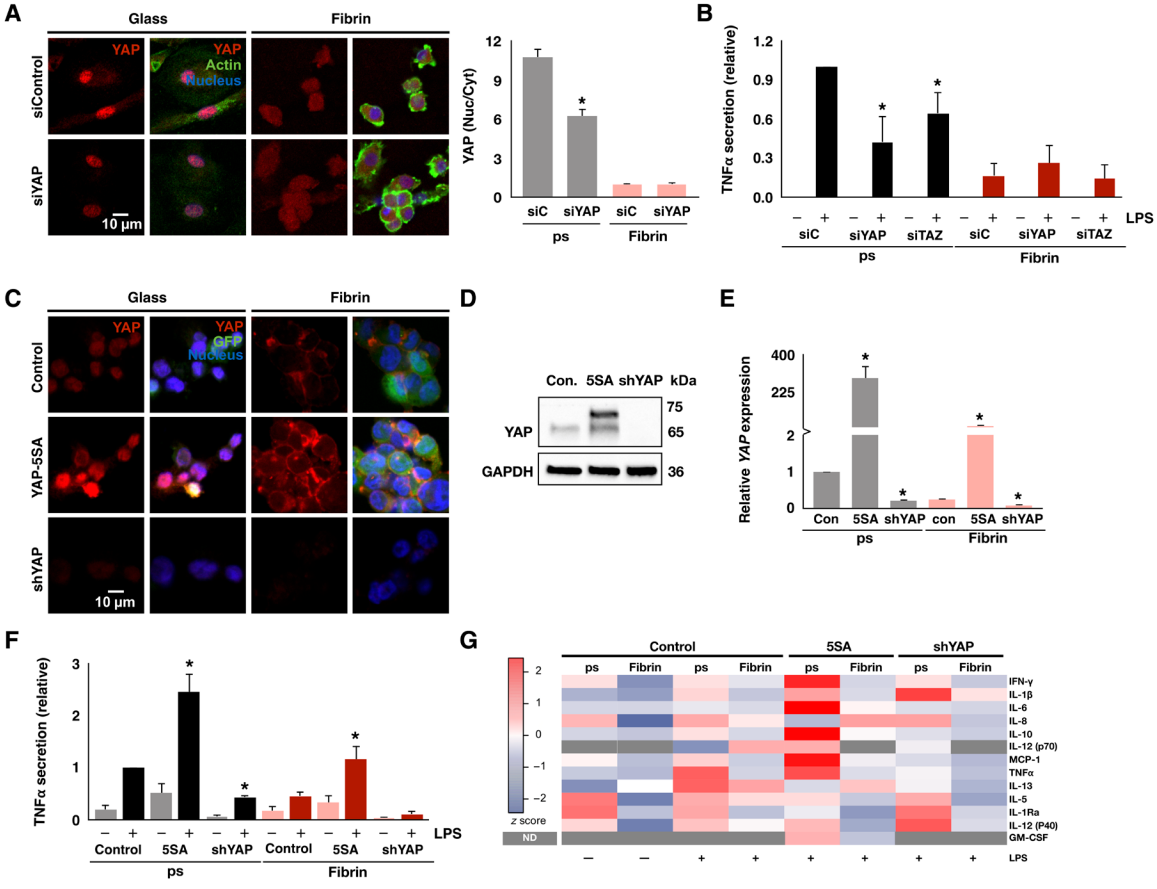

Fig. 4. Nuclear YAP potentiates inflammatory activation of macrophages. (**A**) Immunofluorescence confocal images of YAP in monocyte-derived macrophages treated with YAP siRNA (siYAP) or nontarget control (siControl or siC) for 48 hours and cultured on glass or fibrin (left) and quantification of nuclear to cytoplasmic ratio of YAP (right). (**B**) Secretion of TNFα from macrophages after knockdown of YAP or TAZ and stimulated with LPS (10 ng/ml), analyzed by ELISA. (**C**) Immunofluorescence confocal images of YAP in YAP-5SA–expressing and shYAP-expressing THP-1 cells or blank lentiviral vector–expressing control cells cultured on glass or fibrin and treated with PMA for 24 hours. GFP, green fluorescent protein. (**D**) Immunoblot of transgene expression. (**E**) *YAP* gene expression analyzed by qPCR of the conditions in (C). (**F**) Secretion of TNFα from cells in (C) stimulated with LPS (10 ng/ml), analyzed by ELISA. (**G**) Secretion of proinflammatory cytokines analyzed by multiplex ELISA using human cytokine array for the cells in (C) stimulated with LPS (10 ng/ml). Data are presented as means ± SEM of three biological replicates; **P* < 0.05 when comparing siYAP, siTAZ, or YAP-5SA or shYAP versus respective controls, assessed by two-tailed Student's *t* test. For multiplex ELISA, data are means of three biological replicates for all the LPS-stimulated conditions. ND, not determined; IFN-γ, interferon-γ; GM-CSF, granulocyte-macrophage colony-stimulating factor.

another monocyte/macrophage cell line, U937 (fig. S8, B to D). To further characterize the effects of YAP manipulation on cytokine secretion, we analyzed the supernatants using multiplex human proinflammatory-focused cytokine array. We found that YAP-5SA–expressing THP-1 cells secreted significantly higher levels of proinflammatory cytokines in response to LPS compared to control and shYAP-expressing cells (Fig. 4G). Together, these data show that modulation of YAP activity tunes the macrophage inflammatory response to LPS, with increased active YAP associated with higher levels of inflammation.

Actin polymerization is required for YAP activity

Since macrophages cultured on fibrin and polystyrene or glass exhibited different morphologies and altered distribution of actin (Figs. 1, C and D, and 2A), we examined whether cytoskeletal polymerization, contractility, and Rho guanosine triphosphatase (GTPase) activity were required for adhesion-dependent YAP nuclear localization and inflammatory activation. We immunostained YAP in cells cultured on glass or fibrin in the presence of inhibitors and found that cytochalasin D, an inhibitor of actin polymerization, reduced YAP nuclear localization, consistent with several other reports (*19*). In contrast, cells cultured with blebbistatin, an inhibitor of myosin phosphorylation and thus cell contractility, or inhibitors of Rac1, RhoA, and Cdc42 had little effect (Fig. 5A and fig. S9, A to D). Cytochalasin D also inhibited TNFα secretion in macrophages cultured on polystyrene and enhanced IL-10 secretion on fibrin, whereas blebbistatin, Y27632, and other GTPase inhibitors had minimal effects (Fig. 5B). Together, these data suggest that actin cytoskeletal integrity, but not contractility, is required for YAP nuclear localization and inflammatory activation of macrophages.

To investigate the converse effects of YAP activity on actin, adhesion structures, and contractility, we evaluated YAP-5SA–expressing and shYAP-expressing THP-1 cells for actin and vinculin and traction forces. We found that overexpression of the active YAP, YAP-5SA, led to a decrease in actin and vinculin staining, while silencing YAP appeared to increase the intensity of these structures (Fig. 5C). These results are consistent with a previous published report wherein YAP enhances the transcriptional target ARHGAP29 (Rho GTPase Activating Protein 29) to negatively regulate actin polymerization (*32*). Measurement of traction forces revealed that YAP-5SA–expressing cells concomitantly decreased their overall forces compared to both control and shYAP-expressing cells (Fig. 5D). Together, these data suggest that while cytoskeletal polymerization is needed for YAP entry

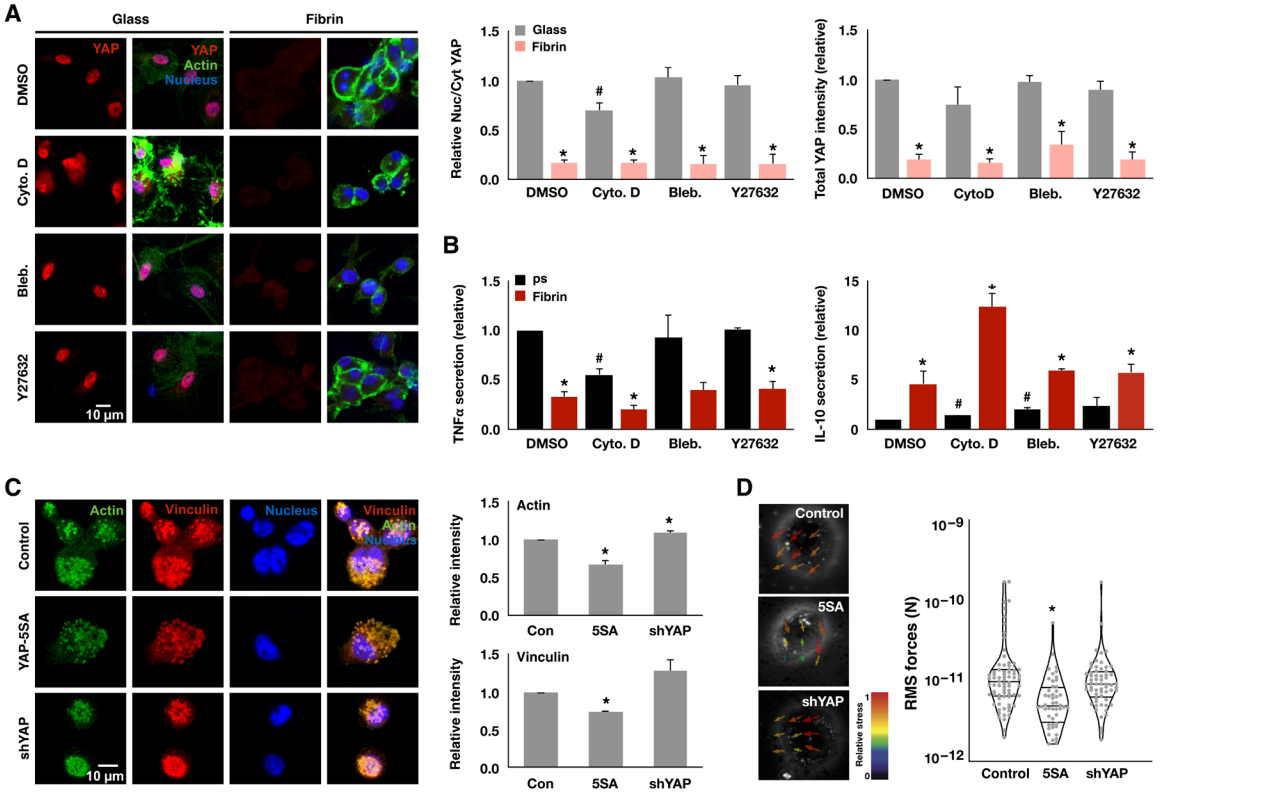

Fig. 5. Actin polymerization is required for YAP, which negatively feeds back to inhibit actin, adhesion, and contractility. (**A**) Immunofluorescence confocal images of YAP in monocyte-derived macrophages, cultured on glass or fibrin hydrogel (2 mg/ml) for 24 hours and treated with indicated cytoskeletal drugs for 6 hours (left), and quantification of YAP nuclear-to-cytoplasmic ratio and total intensity (right). (**B**) Secretion of TNFα and IL-10 secreted from cells in (A) and stimulated with LPS for 6 hours. (**C**) Immunofluorescence confocal images of actin and vinculin in YAP-5SA–expressing and shYAP-expressing THP-1 cells or blank lentiviral vector–transduced control cells cultured on glass overnight (left) and quantification of total actin and vinculin intensity (right). (**D**) Representative bead displacement vectors from particle image velocimetry analysis by traction force microscopy (TFM; left) and quantification of root mean square (RMS) forces of at least 60 cells per condition for YAP-5SA–expressing and shYAP-expressing THP-1 cells or blank lentiviral vector–transduced control cells seeded on 10-kPa polyacrylamide gels. Values are means ± SEM across three biological replicates; **P* < 0.05 when comparing fibrin versus glass or polystyrene or when comparing YAP-5A and shYAP with control and #*P* < 0.05 when comparing drug versus dimethyl sulfoxide (DMSO), assessed by two-tailed Student's *t* test.

into the nucleus, active YAP feeds back to inhibit actin polymerization, adhesion, and contractility within macrophages.

Implant stiffness influences YAP and inflammatory activation in surrounding macrophages

To test whether material stiffness could modulate the function of macrophages, and their YAP activity, in vivo, we transitioned to a murine wound model. We first confirmed that stiffness also modulates YAP activity in murine bone marrow–derived macrophages (fig. S10). We then investigated whether soft environments could modulate YAP and inflammation within wounds by applying fibrin hydrogels (2 mg/ml) to full-thickness excisional wounds created on the dorsal skin of mice. Hydrogels were covered with Tegaderm adhesive, which has a reported elastic modulus of ~8.8 MPa (*33*), and controls consisted of Tegaderm alone. Hematoxylin and eosin (H&E) staining of wound tissue at post-wound day (PWD) 5, revealed expected immune and stromal cell infiltration, with no strong differences in wound architecture between fibrin and Tegaderm treatment (Fig. 6A). However, analysis of scar size in whole-mounted tissues at PWD 30 revealed that fibrin hydrogel application reduced the final scar size of the excisional skin wound, suggesting that manipulation of the mechanical environment during healing influences the resulting scar (Fig. 6B). To examine whether macrophage polarization may be involved in this response, we probed tissue by immunohistochemistry at PWD 5, a time point that we have previously found to exhibit prominent macrophage marker expression.

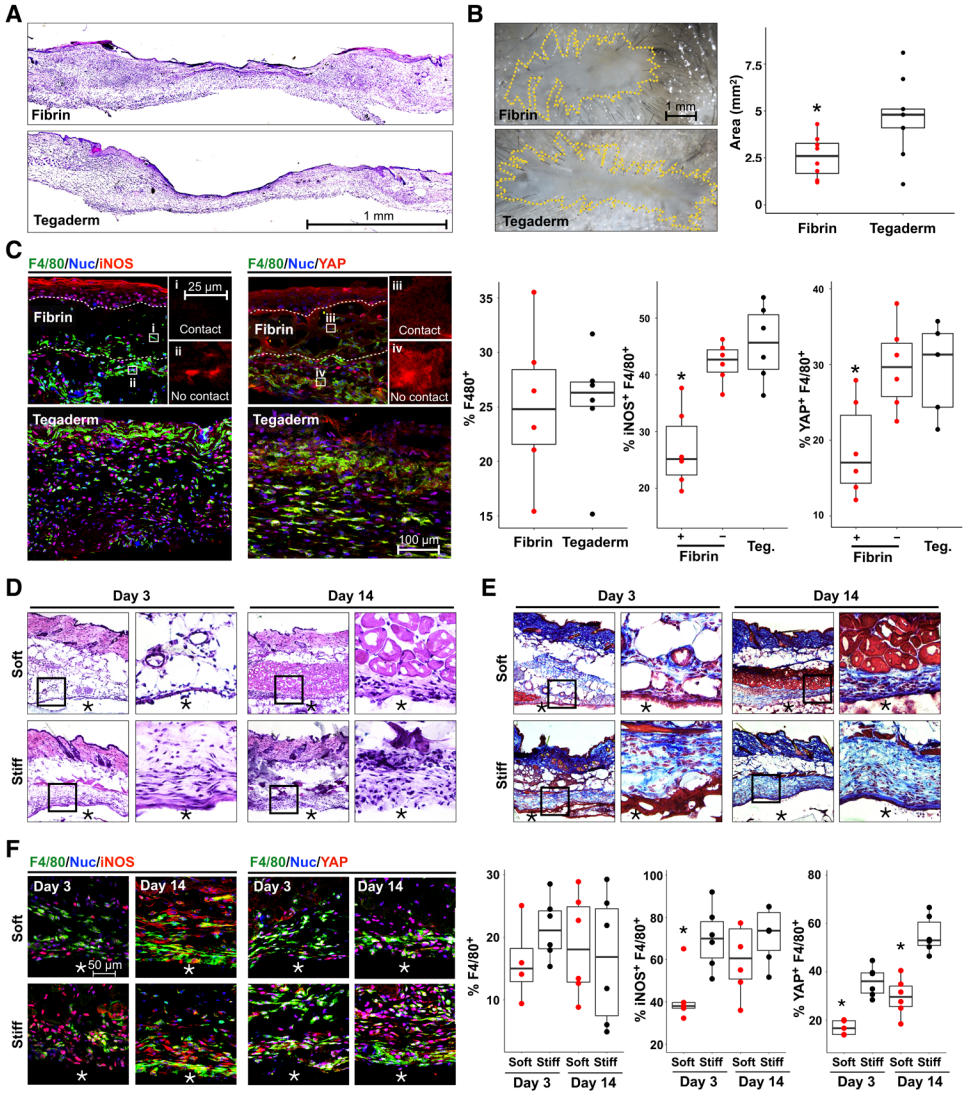

Fig. 6. Biomaterials modulate macrophage YAP and inflammatory activation in vivo. (**A**) H&E of fibrin- and Tegaderm-treated wounds, at PWD 5. (**B**) Micrographs of whole-mount scar tissue at PWD 30 and scar size quantification. (**C**) Confocal images of iNOS (inflammatory marker), YAP, and F4/80 (macrophage marker) in wound tissue at PWD 5 and quantification of %F4/80$^+$ cells, %F4/80$^+$ YAP$^+$, and %F4/80$^+$ iNOS$^+$. (i to iv) Insets show representative cells in contact or not in contact with fibrin gels, which are labeled as + or – fibrin, respectively, in graphs on the right. (**D** and **E**) Representative tissue sections surrounding subcutaneously implanted soft (1 kPa) and stiff (140 kPa) PEGDA hydrogels for 3 or 14 days, stained with H&E (D) or Masson's trichrome (E). (**F**) Confocal images of immunohistochemistry and quantification as in (C), for soft and stiff implants after 3 and 14 days. The asterisks (*) indicate hydrogel material in (D to F). $n \geq 5$ animals and $^*P < 0.05$ when comparing fibrin contact versus no contact or Tegaderm (C) or soft versus stiff (F), assessed by two-tailed Student's t test. Photo credit: Raji Nagalla, University of California, Irvine.

We probed for YAP and inducible nitric oxide synthase (iNOS), an intracellular inflammatory marker. We found a similar percentage of macrophages ($F4/80^+$) in fibrin- and Tegaderm-treated wounds, but uncovered a fibrin contact–dependent reduction in YAP and iNOS (Fig. 6C). More specifically, macrophages that were in contact with the fibrin hydrogel exhibited reduced YAP and iNOS expression, but macrophages that were not in contact expressed similar amounts of YAP and iNOS to macrophages in the Tegaderm-only control (Fig. 6C). These data provide further evidence that biophysical cues regulate macrophage YAP and inflammatory response.

To more specifically test the effects of stiffness, we used photocrosslinkable synthetic PEG diacrylate (PEGDA) hydrogels at 10% (w/v; 1 kPa) and 50% (w/v; 140 kPa). We implanted soft and stiff hydrogels into the dorsal subcutaneous space of C57BL/6J mice. At 3 and 14 days after material implantation, tissue surrounding the hydrogel was harvested and examined by histology and immunohistochemistry. H&E staining revealed increased cell recruitment to stiff implants at 3 and 14 days, compared to soft implants, and Masson's trichrome staining showed increased collagen deposition in response to stiff implants at 14 days (Fig. 6, D and E). Using immunohistochemistry, macrophages were again identified by F4/80 staining and then evaluated for expression of iNOS and YAP (Fig. 6F). Recruitment of $F4/80^+$ macrophages was similar between stiff and soft implants, although the stiff gels trended higher than soft implants at 3 days. We observed higher percent $iNOS^+$ macrophages present within tissue surrounding stiff implants when compared to soft hydrogels at 3 days after implantation, suggesting that stiffness increases the inflammatory response to implanted materials. Furthermore, we observed increased percent YAP^+ macrophages surrounding stiff implants at both 3 and 14 days after implantation, consistent with the effects observed in our in vitro studies. Percent $iNOS^+$ macrophages increased at 14 days, potentially reflecting a continuing foreign body response. This study suggests that manipulation of the biomaterial stiffness alters the inflammatory state and YAP signaling of macrophages.

DISCUSSION

Macrophages have been shown to be sensitive to their physical environment (*34*), but the molecular mechanism underlying these responses has remained relatively unknown. Our studies reveal a role for YAP in macrophage sensing of the stiffness of the environment, tuning their ability to be activated by soluble signals. YAP has been reported to have a minimal role in hematopoietic cells, concomitant with its low expression levels. We indeed find that YAP expression is low in monocytes, but its expression notably increases upon differentiation to adherent macrophages with M-CSF. Furthermore, as differentiated macrophages adhere to culture dishes or glass coverslips, YAP dynamically enters the nucleus and is associated with an increased ability to respond to inflammatory signals, including LPS. Together, our data suggest that dynamic interactions with their physical environment profoundly influence the macrophage response to soluble agonists.

YAP has been implicated in mechanosensation in several other cell types, including endothelial cells, epithelial cells, fibroblasts, and mesenchymal stem cells among others. In most of these cell types, soft environments, cellular confinement, and inhibition of cytoskeletal polymerization and contractility all reduce YAP activity. We show that soft environments and inhibition of actin polymerization with cytochalasin D also inhibit YAP in macrophages. However, confinement through cell micropatterning or culture at confluence, and inhibition of contractility with pharmacological inhibitors of myosin or RhoA signaling, did not reduce YAP in macrophages. In addition, canonical YAP target genes were not up-regulated under conditions where nuclear YAP was observed, suggesting that regulation of YAP in macrophages may be unique. The lack of effects of confinement may be attributed to the function of immune cells such as macrophages, which often are recruited en masse and activated within densely packed tissues.

Our studies show that active YAP potentiates inflammatory activation. These results are consistent with a recent study in Kupffer cells (*35*) and THP-1 cells (*36*) demonstrating that YAP binds promoters of inflammatory genes via TEAD (TEA Domain family member) motifs. Furthermore, a study in Kupffer cells found that LPS stimulation enhances YAP expression, which was also observed in our studies, although we show a much more substantial increase upon adhesion to stiff surfaces. Cross-talk between Hippo-YAP and the inflammation-related NF-κB signaling pathway has been reported, but the interactions appear to vary with cell type and disease conditions (*37*, *38*). The intensity of nuclear YAP was also correlated with the histone marks associated with accessible chromatin states, suggesting that YAP may activate target genes through modification of DNA organization, potentially through histone methyltransferases, as has been shown in other contexts (*39*). Further studies will be needed to investigate whether interactions among YAP, DNA-modifying enzymes, and NF-κB in the nucleus synergistically enhance inflammatory gene transcription in macrophages. Nonetheless, tuning YAP directly or through manipulation of environment stiffness may be an effective therapeutic approach to modulate inflammation during disease.

MATERIALS AND METHODS

Hydrogel fabrication

Fibrin hydrogel substrates were fabricated at 2 mg/ml by mixing soluble fibrinogen from human plasma (EMD Millipore, 341576) mixed with human thrombin (0.4 U/ml; EMD Millipore, 605190) and pipetting it gently into tissue culture wells (with or without glass coverslips) to avoid bubbles. The hydrogels were allowed to form at 37°C for at least 30 min before seeding cells. The collagen gels (2.0 mg/ml) were fabricated using rat tail type I collagen (Corning) according to the manufacturer's protocol. Briefly, collagen was mixed with appropriate amounts of 10× phosphate-buffered saline (PBS; Lonza), 1 M NaOH, and water. Five percent PEGDA hydrogels (200 molecular weight) were made by mixing equal volume of 0.05% Irgacure and 10% PEGDA in PBS. After dispensing the mixture into the well, it was ultraviolet (UV) treated for 10 min. The gels were hydrated with PBS before culturing the cells. Matrigel (Corning) was thawed overnight at 4°C, and depending on the lot concentration, it was diluted to 2 mg/ml with cold RPMI media. The gel was dispensed in the culture well and incubated at 37°C before seeding the cells.

Peripheral blood monocyte isolation and macrophage differentiation

Monocytes were isolated from whole blood by density centrifugation using lymphocyte separation media (MP Biomedicals, Santa Ana, CA). Whole blood was collected at the Institute for Clinical and

Translational Science at the University of California, Irvine, through approved protocols with the UCI Institutional Review Board, and informed consent was obtained from all donors. Monocytes were enriched by counterflow elutriation, as previously described (*40*), and the purity was assessed after every isolation by staining for $CD11b^+$ and $CD3^-CD20^-CD56$. Monocytes were differentiated into macrophages with recombinant human M-CSF (25 ng/ml; PeproTech, NJ) for 7 days, with the addition of fresh media with M-CSF at day 3. Human monocyte-derived macrophages were used for experiments on day 7 of culture.

THP-1 and U937 cell culture

The monocytic cell lines THP-1 and U937 were obtained from the American Type Culture Collection and cultured according to the manufacturer's recommendation. Both the cell lines were differentiated for 18 to 42 hours with 20 nM PMA before experiments.

Enzyme-linked immunosorbent assay and immunostaining

After 7 days of cell culture, the cells were dissociated from the plate using cell dissociation buffer and plated either on cover glass or on fibrin. A total of 0.3 million and 0.1 million cells per well were seeded in 12- and 24-well plates, respectively. After 24 hours of culture, the cells were stimulated with ultrapure LPS (10 ng/ml; InvivoGen). Supernatants were collected 6 hours after stimulation for assessment of cytokine secretion by enzyme-linked immunosorbent assay (ELISA) following the manufacturer's protocol (BioLegend). To assess the cytokine secretion from the control, YAP-5SA, and shYAP, the supernatants were collected from the cells cultured on glass and fibrin (2 mg/ml) after 18 hours of adhesion and 6 hours of stimulation with LPS (10 ng/ml). The cell culture supernatants were analyzed using human multiplex cytokine array proinflammatory focused 15-plex (HDF15) from Eve Technologies, AB, Canada. The heatmap was generated using R software and presented using *z* scores calculated for each sample. Furthermore, the cells were immediately fixed in 4% paraformaldehyde (PFA) for 10 min at room temperature (RT). The cells were washed three times with PBS, permeabilized using 0.3% Triton X-100 in PBS, and then incubated in the following primary antibodies overnight at 4°C: YAP antibody (clone G-6; sc-376830, Santa Cruz Biotechnologies), TAZ antibody (clone D-8; sc-518026, Santa Cruz Biotechnologies), NF-κB p65 antibody (clone F-6; sc-8008, Santa Cruz Biotechnologies), H3Ac antibody (EMD Millipore, 06-599), H3K4me3 antibody (EMD Millipore, 07-473), or monoclonal vinculin antibody (Sigma-Aldrich, V9131). Cells were then washed with 2% bovine serum albumin (BSA) in PBS and incubated with secondary antibody Alexa Fluor 594 anti-mouse immunoglobulin G (BioLegend) at RT for 1 hour. Nuclei and actin were stained using Hoechst and Alexa Fluor 488–phalloidin (Invitrogen) or Alexa Fluor Plus 647 Phalloidin (A22287, Fisher Scientific), respectively, diluted in 2% BSA in PBS for 30 min at RT. Last, the cells were washed with PBS and mounted on glass slides using Fluoromount-G (Southern Biotech).

Confocal microscopy and image analysis

Images were captured using a Zeiss 780 LSM confocal microscope at the Optical Biology Core at the UCI. The captured images were analyzed using ImageJ software for nucleo-cytoplasmic localization of YAP or NF-κB. Briefly, cell boundaries were outlined manually, and the nuclear boundaries were defined by using the corresponding 4′,6-diamidino-2-phenylindole–stained image. The total nuclear intensity of YAP was divided by the total intensity of YAP in the cytoplasm to obtain the nuclear-to-cytoplasmic ratio. For each experiment, at least 150 cells were analyzed.

RNA isolation and quantitative real-time PCR

Cells were lysed using TRI Reagent (T9424, Sigma-Aldrich), and RNA was isolated following the manufacturer's protocol. The pellet was briefly air dried, and the RNA was dissolved in diethyl pyrocarbonate–treated water. cDNA was obtained using the High-Capacity cDNA Reverse Transcription Kit from Applied Biosystems (catalog no. 4368814) with 1 μg of total RNA following the manufacturer's protocol. Bio-Rad's SsoFast EvaGreen Supermix was used for quantitative real-time PCR, and a total of 40 cycles were performed on Bio-Rad's CFX96 real-time PCR system. Relative gene expression was analyzed by $2^{-\Delta\Delta CT}$ method and expressed relative to the housekeeping gene *RPL37A*. The primers used for quantitative PCR in this study include *TNF* (forward, AGGCGCTCCCCAAGAAGACAGG and reverse, CAGCAGGCAGAAGAGCGTGGTG), *IL6* (forward, AAGCCAGAGCTGTGCAGATGAGTA and reverse, CTTGGTCACCGACGTCCTGT), *MCP1* (forward, CCCCAGTCCCTGCTGTTAT and reverse, TGGAATCCTGAACCCACTTC), *IL10* (forward, TCATTCCCCAACCACTTCAT and reverse, GTAGAGACGGGGTTTCACCA), *YAP* (forward, GCAGTTGGGAGCTGTTTCTC and reverse, GCCATGTTGTTGTCTGATCG), *CYR61* (forward, TCACCCTTCTCCACTTGACC and reverse, AGTTTTGCTGCAGTCCTCGT), *AREG* (forward, CTGGGAAGCGTGAACCATTTT and reverse, TCTGAGTAGTCATAGTCGGCTC), *ANKRD1* (forward, GAACTGGTCACTGGAAAGAAGAATG and reverse, GGTGGGCTAGAAGTGTCTTCAGA), and *RPL37A* (forward, ATTGAAATCAGCCAGCACGC and reverse, AGGAACCACAGTGCCAGATCC).

Western blotting

Cells were lysed using radioimmunoprecipitation assay lysis buffer (VWR) supplemented with 1× of Halt protease and phosphatase inhibitor cocktail (Thermo Fisher Scientific). Twenty micrograms of total protein was resolved on 4 to 15% Mini-PROTEAN TGX precast gels (Bio-Rad). Protein was blotted onto nitrocellulose membrane and using iBlot2 transfer systems (Invitrogen). Blots were incubated with primary antibody for 1 hour at RT, and after three washes, it was further incubated with horseradish peroxidase–conjugated secondary for 1 hour. Then, the blot was incubated in SuperSignal West Femto Maximum Sensitivity Substrate (Thermo Fisher Scientific) for 5 min before imaging the blot using Bio-Rad ChemiDoc XRS+ with Image Lab software.

Polyacrylamide gel fabrication and fibrinogen conjugation

Polyacrylamide hydrogels with tunable mechanical properties were synthesized according to the previously described protocol on glass coverslips (*29*). The polyacrylamide-coated glass coverslips were conjugated with fibrinogen (250 μg/ml) using sulfo-SANPAH (Thermo Fisher Scientific) at RT for 2 hours. Cells were cultured for 24 hours on the gel and either fixed immediately for immunostaining or stimulated with LPS (10 ng/ml) for 6 hours for analysis of supernatant by ELISA.

RNA interference

Knockdown of YAP and TAZ was performed by nucleofection (4D-Nucleofector system, Lonza) using siRNAs (Dharmacon). The sequences of siRNA used in this study are as follows: *YAP* siRNA

smart pool (GGUCAGAGAUACUUCUUAA, CCACCAAGCUAGAUAAAGA, GAACAUAGAAGGAGAGGAG, and GCACCUAUCCUCUCGAGA), *TAZ* siRNA (GACAUGAGAUCCAUCACUA), and nontarget siRNA (UAAGGCUAUGAAGAGAUAC). Briefly, 0.5 million freshly isolated monocytes were transfected with 100 nM corresponding siRNAs in 20 μl of nucleofection solution. After nucleofection, cells were recovered in RPMI 1640 complete media [10% heat-inactivated fetal bovine serum + 1% penicillin and streptomycin + 10% M-CSF] for 42 hours and stimulated with LPS (10 ng/ml). Cells were immunostained, and supernatant was analyzed as described earlier.

Lentiviral transduction

YAP-5SA, shYAP, and control lentiviral transfer plasmids were generated by transient transfection of human embryonic kidney 293T cells. Supernatants were concentrated and then used to transfect THP-1 and U937 cells. One million THP-1 or U937 cells were mixed with 2 ml of lentiviral supernatant and hexadimethrine bromide (8 μg/ml; Polybrene, Sigma-Aldrich) and spun at 2500 rpm for 2 hours at RT. After 24 hours, the cells were spun again and resuspended in THP-1/U937 media with puromycin (2 μg/ml).

Cytoskeletal inhibitors

Cytoskeleton inhibitor drugs were added to cells after 24 hours of cell seeding for 30 min, followed by 6-hour stimulation with 10 ng of LPS. Supernatants were analyzed for secreted cytokines by ELISA, and the cells were fixed and stained as described above. The drugs and the concentration used in this study are cytochalasin D (10 μM; potent inhibitor of actin polymerization), blebbistatin [30 μM; myosin inhibitor, specific for myosin II), Y-27632 [30 μM; ROCK (Rho-associated protein kinase) inhibitor], Rho II Y16 [15 μM; Rho inhibitor II, targets Rho guanine nucleotide exchange factors (RhoGEFs)], Rac1 (100 μM; Rac1 inhibitor, inhibits Rac1 guanosine diphosphate/guanosine triphosphate exchange activity), and Cdc42 III (50 μM; Cdc42 inhibitor III, targets Cdc42 GEF).

Traction force microscopy

For traction force microscopy (TFM), polyacrylamide gel substrates were prepared with a modified procedure of previously published protocols (*29*, *41*). Briefly, glass bottom dishes (35 mm) were UV-ozone–treated and functionalized using 0.3% (v/v) 3-(trimethoxysilyl) propyl methacrylate (Sigma-Aldrich). Glass coverslips functionalized with poly-D-lysine (0.1 mg/ml; Gibco) were coated with 1:800 (v/v) aqueous dilution of red fluorescent microspheres (0.5 μm, carboxylate modified; Thermo Fisher Scientific) (*41*). Gels (10 kPa) were prepared by sandwiching polymerizing acrylamide-bisacrylamide solution on the functionalized glass bottom dishes with microsphere-coated coverslips. After polymerization, the coverslips were peeled off, and fibronectin (20 μg/ml) was conjugated to the surface of gels with sulfo-SANPAH reagent (Thermo Fisher Scientific). After disinfecting the surface with UV light for 30 min, cells were seeded at 20,000 cells per dish. TFM imaging was performed by capturing images of microbeads and cell location at 24 hours after seeding. The cells were released from the gel surface with a 0.1% SDS solution. Fiji software was used to register any unaligned images. Subsequently, particle image velocimetry and Fourier transform traction cytometry were performed as previously described (*42*). A custom code was written in Python and IJ1 macro language to batch process the single-cell traction forces. The root mean square forces are calculated as the square root of the mean squared forces associated with the bead displacement by single cells, measured using 24-pixel interrogation windows. At least 60 individual cells per condition were analyzed.

Animal studies

Animal use, husbandry, and wounding were approved by the Institutional Animal Care and Use Committee of University of California, Irvine.

Full-thickness excisional skin wounding study

Full-thickness skin wounding was carried out on p50 C57BL/6 mice. Mice were anesthetized using isoflurane and shaved; p50 mice were chosen to minimize the impact of anagen phase hair follicles during wound healing. Dorsal skin was cleansed using 70% ethanol, and a single full-thickness wound was made with 5-mm biopsy punches at the dorsal midline, immediately below the scapulae. This location was chosen to minimize disruption to the wound during healing. Wounds were treated with either 20 μl of saline or 10 μl of bovine thrombin (Sigma-Aldrich) and 10 μl of bovine fibrinogen (EMD Millipore) to a final concentration of fibrin at 8 mg/ml and thrombin at 4 U/ml. After allowing 1 min for gelation, wounds were dressed with Tegaderm followed by two ¾"x2" adhesive bandages. Mice were housed individually after wounding and monitored daily for signs of infection/healing. At 5 or 30 days after wounding, mice were sacrificed and dressings were carefully removed. Wounded skin was excised with a ≥5-mm margin and mounted in OCT (optimal cutting temperature solution) for cryosectioning or fixed in 4% PFA for whole-mount imaging.

Subcutaneous implant study

PEGDA gel implants were carried out on adult (22 weeks old) C57BL/6J mice. PEGDA (400 MW; Polysciences Inc.) was reconstituted in PBS at 50% (for stiff 140-kPa implants) or 10% (w/v; for soft 1-kPa implants), with 0.005% Irgacure 2959 photoinitiator. One-millimeter sheets were cast and cross-linked with UV for 5 min, and then, 5-mm biopsy punches were used to create disks for implantation. Mice were anesthetized using isoflurane; dorsal skin was shaved and cleansed using 70% ethanol, and a ~5-mm incision was made along the dorsal midline, immediately below the scapulae. A subcutaneous pocket was dissected on each side laterally, and soft and stiff PEGDA gels were placed inside, one on each side. The incision was closed using staples. Mice were housed individually after wounding and given acetaminophen in their drinking water ad libitum. Mice were monitored daily for signs of infection/healing. At 3 or 14 days after implant, mice were sacrificed; implants were retrieved with surrounding tissue and mounted in OCT for cryosectioning.

Immunohistochemistry

Frozen tissue sections were thawed to RT, fixed in 4% PFA for 15 min, and then washed four times with PBS. Tissues were permeabilized with 0.1% Triton X-100 (Sigma-Aldrich) and then washed three times with PBS 0.1% Tween 20 (Sigma-Aldrich), before blocking in 1% BSA + 0.1% Tween for 2 hours. Sections were stained for F4/80 (BM8, Thermo Fisher Scientific), YAP (14074S, Cell Signaling Technology), and iNOS (651, Santa Cruz Biotechnology or 15323, Abcam) overnight at 4°C. Slides were then washed three times with PBS 0.1% Tween 20 and then stained for 1 hour with fluorescent-conjugated secondary antibodies (A21209, A21244, and A21206, respectively, Thermo Fisher Scientific). After washing three times with PBS 0.1% Tween-20, 5 min each, slides were mounted with

Fluoromount-G and imaged at 20× using the Olympus FV3000 laser scanning confocal microscope.

SUPPLEMENTARY MATERIALS

Supplementary material for this article is available at http://advances.sciencemag.org/cgi/content/full/6/49/eabb8471/DC1

View/request a protocol for this paper from *Bio-protocol*.

REFERENCES AND NOTES

1. T. A. Wynn, A. Chawla, J. W. Pollard, Macrophage biology in development, homeostasis and disease. *Nature* **496**, 445–455 (2013).
2. T. A. Wynn, K. M. Vannella, Macrophages in tissue repair, regeneration, and fibrosis. *Immunity* **44**, 450–462 (2016).
3. P. Lu, K. Takai, V. M. Weaver, Z. Werb, Extracellular matrix degradation and remodeling in development and disease. *Cold Spring Harb. Perspect. Biol.* **3**, a005058 (2011).
4. J. Y. Hsieh, T. D. Smith, V. S. Meli, T. N. Tran, E. L. Botvinick, W. F. Liu, Differential regulation of macrophage inflammatory activation by fibrin and fibrinogen. *Acta Biomater.* **47**, 14–24 (2017).
5. B.-H. Cha, S. R. Shin, J. Leijten, Y.-C. Li, S. Singh, J. C. Liu, N. Annabi, R. Abdi, M. R. Dokmeci, N. E. Vrana, A. M. Ghaemmaghami, A. Khademhosseini, Integrin-mediated interactions control macrophage polarization in 3D hydrogels. *Adv. Healthc. Mater.* **6**, (2017).
6. A. K. Blakney, M. D. Swartzlander, S. J. Bryant, The effects of substrate stiffness on the in vitro activation of macrophages and in vivo host response to poly(ethylene glycol)-based hydrogels. *J. Biomed. Mater. Res. A* **100**, 1375–1386 (2012).
7. M. L. Previtera, A. Sengupta, Substrate stiffness regulates proinflammatory mediator production through TLR4 activity in macrophages. *PLOS ONE* **10**, e0145813 (2015).
8. P. P. Provenzano, P. J. Keely, Mechanical signaling through the cytoskeleton regulates cell proliferation by coordinated focal adhesion and Rho GTPase signaling. *J. Cell Sci.* **124**, 1195–1205 (2011).
9. Z. Sun, S. S. Guo, R. Fassler, Integrin-mediated mechanotransduction. *J. Cell Biol.* **215**, 445–456 (2016).
10. J. Árnadóttir, M. Chalfie, Eukaryotic mechanosensitive channels. *Annu. Rev. Biophys.* **39**, 111–137 (2010).
11. D. Choquet, D. P. Felsenfeld, M. P. Sheetz, Extracellular matrix rigidity causes strengthening of integrin–cytoskeleton linkages. *Cell* **88**, 39–48 (1997).
12. N. Wang, Review of cellular mechanotransduction. *J. Phys. D Appl. Phys.* **50**, 233002 (2017).
13. J. D. Humphrey, E. R. Dufresne, M. A. Schwartz, Mechanotransduction and extracellular matrix homeostasis. *Nat. Rev. Mol. Cell Biol.* **15**, 802–812 (2014).
14. S. Seetharaman, S. Etienne-Manneville, Integrin diversity brings specificity in mechanotransduction. *Biol. Cell* **110**, 49–64 (2018).
15. S. Dupont, L. Morsut, M. Aragona, E. Enzo, S. Giulitti, M. Cordenonsi, F. Zanconato, J. Le Digabel, M. Forcato, S. Bicciato, N. Elvassore, S. Piccolo, Role of YAP/TAZ in mechanotransduction. *Nature* **474**, 179–183 (2011).
16. S. Dupont, Role of YAP/TAZ in cell-matrix adhesion-mediated signalling and mechanotransduction. *Exp. Cell Res.* **343**, 42–53 (2016).
17. P. A. Janmey, R. G. Wells, R. K. Assoian, C. A. McCulloch, From tissue mechanics to transcription factors. *Differentiation* **86**, 112–120 (2013).
18. S. Piccolo, S. Dupont, M. Cordenonsi, The biology of YAP/TAZ: Hippo signaling and beyond. *Physiol. Rev.* **94**, 1287–1312 (2014).
19. K.-I. Wada, K. Itoga, T. Okano, S. Yonemura, H. Sasaki, Hippo pathway regulation by cell morphology and stress fibers. *Development* **138**, 3907–3914 (2011).
20. L. Jansson, J. Larsson, Normal hematopoietic stem cell function in mice with enforced expression of the Hippo signaling effector YAP1. *PLOS ONE* **7**, e32013 (2012).
21. E. Donato, F. Biagioni, A. Bisso, M. Caganova, B. Amati, S. Campaner, YAP and TAZ are dispensable for physiological and malignant haematopoiesis. *Leukemia* **32**, 2037–2040 (2018).
22. C. Lee-Thedieck, J. P. Spatz, Biophysical regulation of hematopoietic stem cells. *Biomater. Sci.* **2**, 1548–1561 (2014).
23. K.-C. Wang, Y.-T. Yeh, P. Nguyen, E. Limqueco, J. Lopez, S. Thorossian, K.-L. Guan, Y.-S. J. Li, S. Chien, Flow-dependent YAP/TAZ activities regulate endothelial phenotypes and atherosclerosis. *Proc. Natl. Acad. Sci. U.S.A.* **113**, 11525–11530 (2016).
24. Y.-J. Huang, C.-K. Yang, P.-L. Wei, T.-T. Huynh, J. Whang-Peng, T.-C. Meng, M. Hsiao, Y.-M. Tzeng, A. T. H. Wu, Y. Yen, Ovatodiolide suppresses colon tumorigenesis and prevents polarization of M2 tumor-associated macrophages through YAP oncogenic pathways. *J. Hematol. Oncol.* **10**, 60 (2017).
25. Y. Feng, Y. Liang, X. Zhu, M. Wang, Y. Gui, Q. Lu, M. Gu, X. Xue, X. Sun, W. He, J. Yang, R. L. Johnson, C. Dai, The signaling protein Wnt5a promotes TGFβ1-mediated macrophage polarization and kidney fibrosis by inducing the transcriptional regulators Yap/Taz. *J. Biol. Chem.* **293**, 19290–19302 (2018).
26. R. Johnson, G. Halder, The two faces of Hippo: Targeting the Hippo pathway for regenerative medicine and cancer treatment. *Nat. Rev. Drug Discov.* **13**, 63–79 (2014).
27. F. Zanconato, M. Cordenonsi, S. Piccolo, YAP/TAZ at the roots of cancer. *Cancer Cell* **29**, 783–803 (2016).
28. T. Lawrence, The nuclear factor NF-κB pathway in inflammation. *Cold Spring Harb. Perspect. Biol.* **1**, a001651 (2009).
29. J. R. Tse, A. J. Engler, Preparation of hydrogel substrates with tunable mechanical properties. *Curr. Protoc. Cell Biol.* **47**, 10.16.1–10.16.16 (2010).
30. A. Elosegui-Artola, I. Andreu, A. E. M. Beedle, A. Lezamiz, M. Uroz, A. J. Kosmalska, R. Oria, J. Z. Kechagia, P. Rico-Lastres, A.-L. Le Roux, C. M. Shanahan, X. Trepat, D. Navajas, S. Garcia-Manyes, P. Roca-Cusachs, Force triggers YAP nuclear entry by regulating transport across nuclear pores. *Cell* **171**, 1397–1410.e14 (2017).
31. J. Y. Lee, J. K. Chang, A. A. Dominguez, H. P. Lee, S. Nam, J. Chang, S. Varma, L. S. Qi, R. B. West, O. Chaudhuri, YAP-independent mechanotransduction drives breast cancer progression. *Nat. Commun.* **10**, 1848 (2019).
32. Y. Qiao, J. Chen, Y. B. Lim, M. L. Finch-Edmondson, V. P. Seshachalam, L. Qin, T. Jiang, B. C. Low, H. Singh, C. T. Lim, M. Sudol, YAP regulates actin dynamics through ARHGAP29 and promotes metastasis. *Cell Rep.* **19**, 1495–1502 (2017).
33. B. Yu, S.-Y. Kang, A. Akthakul, N. Ramadurai, M. Pilkenton, A. Patel, A. Nashat, D. G. Anderson, F. H. Sakamoto, B. A. Gilchrest, R. R. Anderson, R. Langer, An elastic second skin. *Nat. Mater.* **15**, 911–918 (2016).
34. V. S. Meli, P. K. Veerasubramanian, H. Atcha, Z. Reitz, T. L. Downing, W. F. Liu, Biophysical regulation of macrophages in health and disease. *J. Leukoc. Biol.* **106**, 283–299 (2019).
35. K. Song, H. Kwon, C. Han, W. Chen, J. Zhang, W. Ma, S. Dash, C. R. Gandhi, T. Wu, YAP in Kupffer cells enhances the production of pro-inflammatory cytokines and promotes the development of non-alcoholic steatohepatitis. *Hepatology* **72**, 72–78 (2019).
36. X. Zhou, W. Li, S. Wang, P. Zhang, Q. Wang, J. Xiao, C. Zhang, X. Zheng, X. Xu, S. Xue, L. Hui, H. Ji, B. Wei, H. Wang, YAP aggravates inflammatory bowel disease by regulating M1/M2 macrophage polarization and gut microbial homeostasis. *Cell Rep.* **27**, 1176–1189.e5 (2019).
37. Y. Gao, Y. Yang, F. Yuan, J. Huang, W. Xu, B. Mao, Z. Yuan, W. Bi, TNFα-YAP/p65-HK2 axis mediates breast cancer cell migration. *Oncogenesis* **6**, e383 (2017).
38. Y. Deng, J. Lu, W. Li, A. Wu, X. Zhang, W. Tong, K. K. Ho, L. Qin, H. Song, K. K. Mak, Reciprocal inhibition of YAP/TAZ and NF-κB regulates osteoarthritic cartilage degradation. *Nat. Commun.* **9**, 4564 (2018).
39. R. E. Hillmer, B. A. Link, The roles of hippo signaling transducers Yap and Taz in chromatin remodeling. *Cell* **8**, 502 (2019).
40. L. Gov, C. A. Schneider, T. S. Lima, W. Pandori, M. B. Lodoen, NLRP3 and potassium efflux drive rapid IL-1β release from primary human monocytes during *Toxoplasma gondii* infection. *J. Immunol.* **199**, 2855–2864 (2017).
41. S. G. Knoll, M. Y. Ali, M. T. Saif, A novel method for localizing reporter fluorescent beads near the cell culture surface for traction force microscopy. *J. Vis. Exp.* , 51873 (2014).
42. Q. Tseng, E. Duchemin-Pelletier, A. Deshiere, M. Balland, H. Guillou, O. Filhol, M. Thery, Spatial organization of the extracellular matrix regulates cell–cell junction positioning. *Proc. Natl. Acad. Sci. U.S.A.* **109**, 1506–1511 (2012).

Acknowledgments: We acknowledge T. A. Phan for providing the method for TFM and the code for analysis. **Funding:** This work was supported by the NIH National Institute of Allergy and Infectious Disease (NIAID) Grant R21AI128519, National Institute of Dental and Craniofacial Research (NIDCR) Grant DP2DE023319, and National Institute of Arthritis and Musculoskeletal and Skin Diseases (NIAMS) Grant R21AR077288-01 to W.F.L.; a National Institute of Biomedical Imaging and Bioengineering (NIBIB) Grant R21EB027840 to W.F.L. and T.L.D.; a Pilot Project Award from NIAMS P30AR075047 to W.F.L. and M.V.P.; NIAMS Grant U01AR073159, Pew Charitable Trust and LEO Foundation Grants to M.V.P.; a National Institute of General Medical Sciences Grant GM126048 to W.W.; a NIAID Grant R01AI120846 to M.B.L.; and an NSF grant (DMS1763272) and a grant from the Simons Foundation (594598 QN) to T.L.D and M.V.P. H.A. was supported by NIH National Institute T32 Training Grant in Cardiovascular Applied Research and Entrepreneurship (5T32 HL116270-3) and an American Heart Association Predoctoral Fellowship (20PRE35200220). R.R.N. was supported by a UC Irvine Medical Scientist Training Program NIH training grant (T32 GM008620-18) and NIH NIAID F30 fellowship (AI142988-01A1). C.F.G-J. is supported by UC Irvine Chancellor's ADVANCE Postdoctoral Fellowship Program, NSF-Simons Postdoctoral Fellowship, and by a kind gift from the Howard Hughes Medical Institute Hanna H. Gray Postdoctoral Fellowship Program. **Author contributions:** V.S.M., D.A.F.,

W.W., and W.F.L. conceived the project and designed the experiments. V.S.M., H.A., P.K.V., T.U.L., and J.Y.H. designed, performed, and analyzed macrophage experiments. R.R.N., C.F.G.-J., K.Y., E.Y.C., and M.V.P. designed, performed, and analyzed wound and implant studies. W.P. and M.B.L. provided monocytes. P.K.V. and T.L.D. designed, performed, and analyzed traction force experiments. V.S.M., D.A.F., M.B.L., M.V.P., W.W., and W.F.L. wrote the manuscript. **Competing interests:** The authors declare that they have no competing interests. **Data and materials availability:** All data needed to evaluate the conclusions in the paper are present in the paper and/or the Supplementary Materials. Additional data related to this paper may be requested from the authors.

Submitted 26 March 2020
Accepted 20 October 2020
Published 4 December 2020
10.1126/sciadv.abb8471

Citation: V. S. Meli, H. Atcha, P. K. Veerasubramanian, R. R. Nagalla, T. U. Luu, E. Y. Chen, C. F. Guerrero-Juarez, K. Yamaga, W. Pandori, J. Y. Hsieh, T. L. Downing, D. A. Fruman, M. B. Lodoen, M. V. Plikus, W. Wang, W. F. Liu, YAP-mediated mechanotransduction tunes the macrophage inflammatory response. *Sci. Adv.* **6**, eabb8471 (2020).